iScience

CellPress
OPEN ACCESS

Article

Development of vessel mimicking microfluidic device for studying mechano-response of endothelial cells

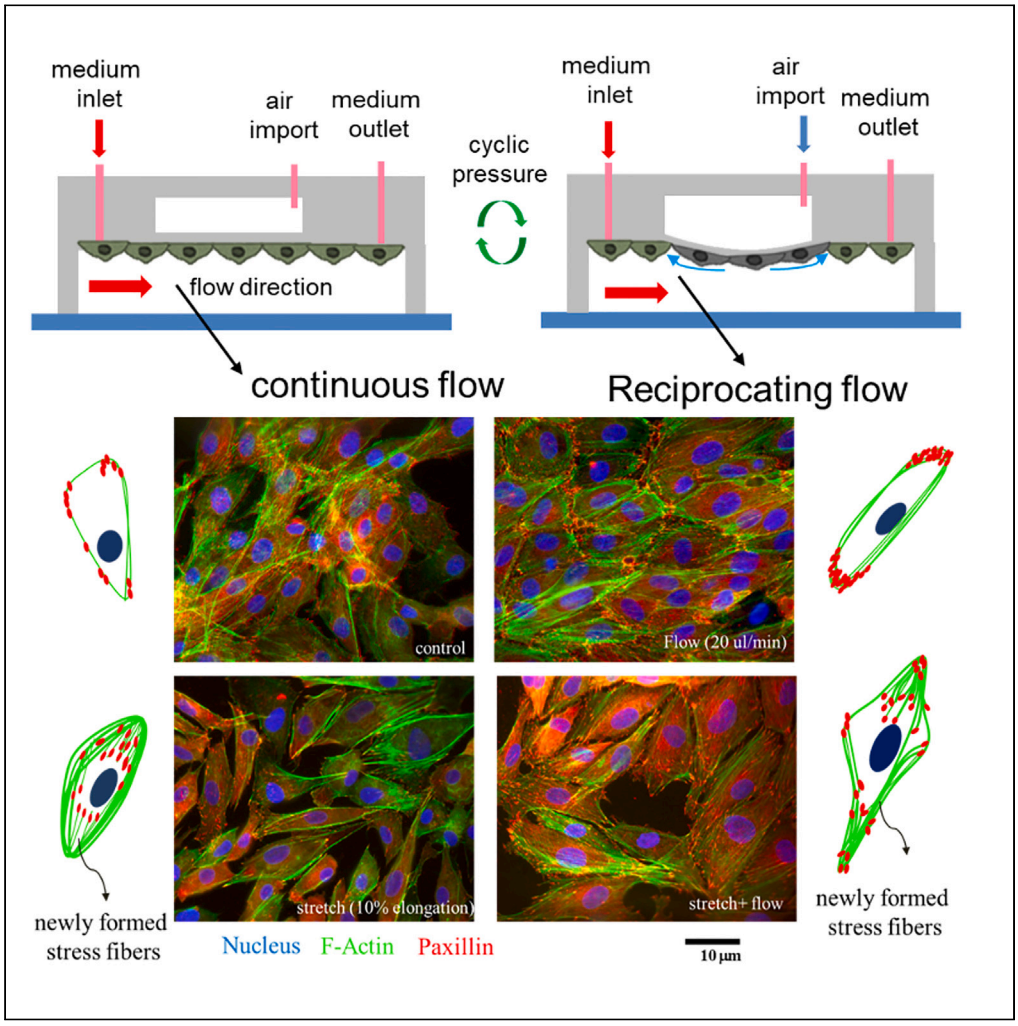

Pei-Yu Chu, Han-Yun Hsieh, Pei-Shan Chung, ..., Yin-Quan Chen, Jean-Cheng Kuo, Yu-Jui Fan

ray.yj.fan@tmu.edu.tw

Highlights

This study is to develop a microfluidic system mimicking arterial blood vessels

Cell behaviors in the system can be monitored in real time

The system mimics arterial environment including pulsatile flow and dynamic stretch

ECs align the cytoskeleton protein and paxillin redistribution under dynamic stretch

Chu et al., iScience 26, 106927
June 16, 2023
https://doi.org/10.1016/j.isci.2023.106927

iScience

CellPress
OPEN ACCESS

Article

Development of vessel mimicking microfluidic device for studying mechano-response of endothelial cells

Pei-Yu Chu,[1,7] Han-Yun Hsieh,[1,3,7] Pei-Shan Chung,[2] Pai-Wen Wang,[3] Ming-Chung Wu,[4] Yin-Quan Chen,[5] Jean-Cheng Kuo,[4,5] and Yu-Jui Fan[1,6,8,*]

SUMMARY

The objective of this study is to develop a device to mimic a microfluidic system of human arterial blood vessels. The device combines fluid shear stress (FSS) and cyclic stretch (CS), which are resulting from blood flow and blood pressure, respectively. The device can reveal real-time observation of dynamic morphological change of cells in different flow fields (continuous flow, reciprocating flow and pulsatile flow) and stretch. We observe the effects of FSS and CS on endothelial cells (ECs), including ECs align their cytoskeleton proteins with the fluid flow direction and paxillin redistribution to the cell periphery or the end of stress fibers. Thus, understanding the morphological and functional changes of endothelial cells on physical stimuli can help us to prevent and improve the treatment of cardiovascular diseases.

INTRODUCTION

Endothelial cells (ECs) within blood vessels form a lining of the interior surface of blood vessels, named as endothelium.[1] Blood flow and blood pressure produce the fluid shear stress (FSS) and cyclic stretch (CS) on the ECs. FSS and CS have been proposed as pathogenic factors of cardiovascular disease. Mechanical forces change the morphology and function of endothelial cells,[2–7] including adhesion,[8–10] migration[11] and cytoskeletal arrangement.[12] Therefore, studying the changes in endothelial cells stimulated by FSS and/or CS will be of great help to the future research of cardiovascular disease and treatment.

The endothelium has the function to maintain blood fluidity and regulate blood clotting. Damaged blood vessel causes the initiation of the hemostatic system, including vascular constriction, platelet plug formation, and blood coagulation. In response to injury or infection, the endothelial cells release chemicals, which regulate platelets activation and the coagulation cascades for maintaining the blood fluidity and preventing thrombosis formation.[13–16] Therefore, the endothelial cells play an indispensable role in the hemostatic system. Healthy endothelial cells inhibit platelets aggregation and regulate fibrinolysis.[17] Endothelial cells injuries and endothelial dysfunction may promote platelet adhesion, aggregation and fibrin formation,[18] causing clot formation and finally the thrombosis. Endothelial dysfunction is initial characteristics of cardiovascular diseases, including hypertension, atherosclerosis, thrombosis, stroke and coronary artery disease.[19] Accordingly, understanding the role of endothelial cells on FSS and/or CS stimulation is crucial for the treatment, prevention of cardiovascular diseases and drug discovery.[20–22]

Several reports have demonstrated the applications of combining mechanical stimuli in the *in vitro* cell culture system. These devices are applied to investigate the role of fluid shear stress or cyclic stretching on the regulation of endothelial cell behavior.[23–30] Ives et al. established a stretch chamber[31] and a constant head steady flow loop[32] *in vitro* models to investigate the effect of cyclic stretch and fluid shear stress on endothelial cells. In addition, Shikata et al. established a cell culture flow system and a FX4000T Flexcell Tension Plus system (Flexcell International, McKeesport, PA) to investigate mechanical stimulation for redistribution of focal adhesions (Fas).[33–35] However, none of the devices are designed to generate and apply FSS or CS on cells. Importantly, the size of these devices may consume large amounts of tissue culture materials.

Other than use these independent designs for studying FSS and CS to endothelial cells, Toda et al. have combined FSS and CS on a system in an *in vitro* model that can be applied to study gene regulation and the changes of morphology under mechanical stimuli.[36] With the development of microfluidics system, the combination of microfluidics and cell culture has gradually emerged. Because the flow of microfluidics is

[1]College of Biomedical Engineering, Taipei Medical University, 250 Wuxing Street, Taipei 11031, Taiwan

[2]Department of Bioengineering, University of California Los Angeles, 420 Westwood Plaza, Los Angeles, CA 90095, USA

[3]Institute of Applied Mechanics, National Taiwan University, No. 1, Sec. 4, Roosevelt Road, Taipei 10617, Taiwan

[4]Institute of Biochemistry and Molecular Biology, National Yang Ming Chiao Tung University, No.155, Sec.2, Linong Street, Taipei 11221, Taiwan

[5]Cancer Progression Research Center, National Yang Ming Chiao Tung University, No.155, Sec.2, Linong Street, Taipei 11221, Taiwan

[6]International Ph.D. Program for Biomedical Engineering, Taipei Medical University, 250 Wuxing Street, Taipei 11031, Taiwan

[7]These authors contributed equally

[8]Lead contact

*Correspondence: ray.yj.fan@tmu.edu.tw

https://doi.org/10.1016/j.isci.2023.106927

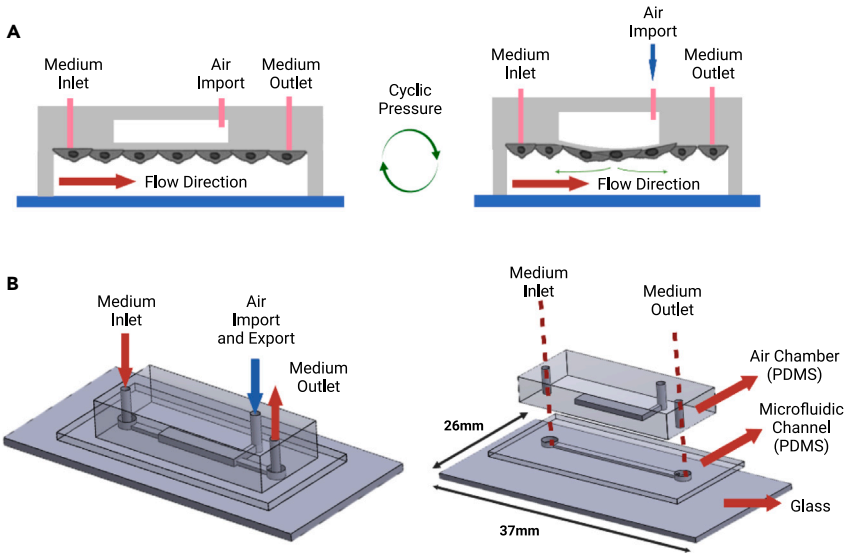

Figure 1. Schematics of the microfluidic shearing-stretching device

(A and B) Cells cultured in microfluidic device with reguler and pressurized mode. These two modes cyclic alternate to stretch cells in the device.

(C and D) The device contains two layers of microfluidic channel/chamber and three inlet/outlets. Two inlet/outlets connect to bottom channel for loading cells and applying shear flow. Upper chamber connects to an air inlet/outlet for cyclically pressurizing to provide cyclic stretch.

mainly laminar flow, and the hydrodynamics simulated by microfluidics system is similar to the microenvironment *in vivo*.[7,37,38] In addition, Zheng et al. have developed a microfluidic flow-stretch chip, which can simultaneously or independently apply FSS and CS to cells to observe the organization of actin stress fibers.[39] After applying one dimensional CS, the actin stress fibers are perpendicularly aligned to the direction of stretching, but the arrangement of cells subjected to FSS is not significantly parallel to the direction of fluid flow.

In this study, we developed a shearing-stretching device to mimic blood vessel, in which the effect of mechanical stimuli on bovine aortic endothelial cells (BAECs) can be observed under microfluidics. This device provided versatile mechano-environments through supplying shear flow and substrate stretching separately or simultaneously, as shown in Figures 1A and 1B. The cells cultured in this device were able to receive different combinations of mechanical forces including pure flow (continuous flow, reciprocating flow, and pulsatile flow), cyclic stretching with reciprocating flow, or cyclic stretching with pulsatile flow. We also investigated cell mechanotransduction on different stiffness materials. The BAECs were cultured on the PDMS and glass to observe the changes of cell morphology under mechanical stimuli. Moreover, cell elongation, arrangement, FAs distribution, and cell size in BAECs under different mechanical stimuli were investigated.

Comparing to most of previous efforts which provided CS in either 1D or 2D direction at a flat surface, this proposed device that are similar to ECs in real vessel presents the CS in radial direction, and curved deformation. This platform is also able to provide several functions that have not yet been studied, such us reciprocating flow dependent/independent with CS that can be used to learn new biology in the future.

RESULTS

Finite element simulations of device

To characterize flow type resulting from combination of continuous flow and reciprocating flow, which is induced by cyclic PDMS deformation, the finite element software, COMSOL, was used to simulate the different combination cases. A 2D model that represents central cross-section area as Figure 2A was built. The upper layer is PDMS membrane, and lower layer is microfluidic channel and material properties of PDMS and water were given, separately. The boundary conditions of PDMS membrane at left and right

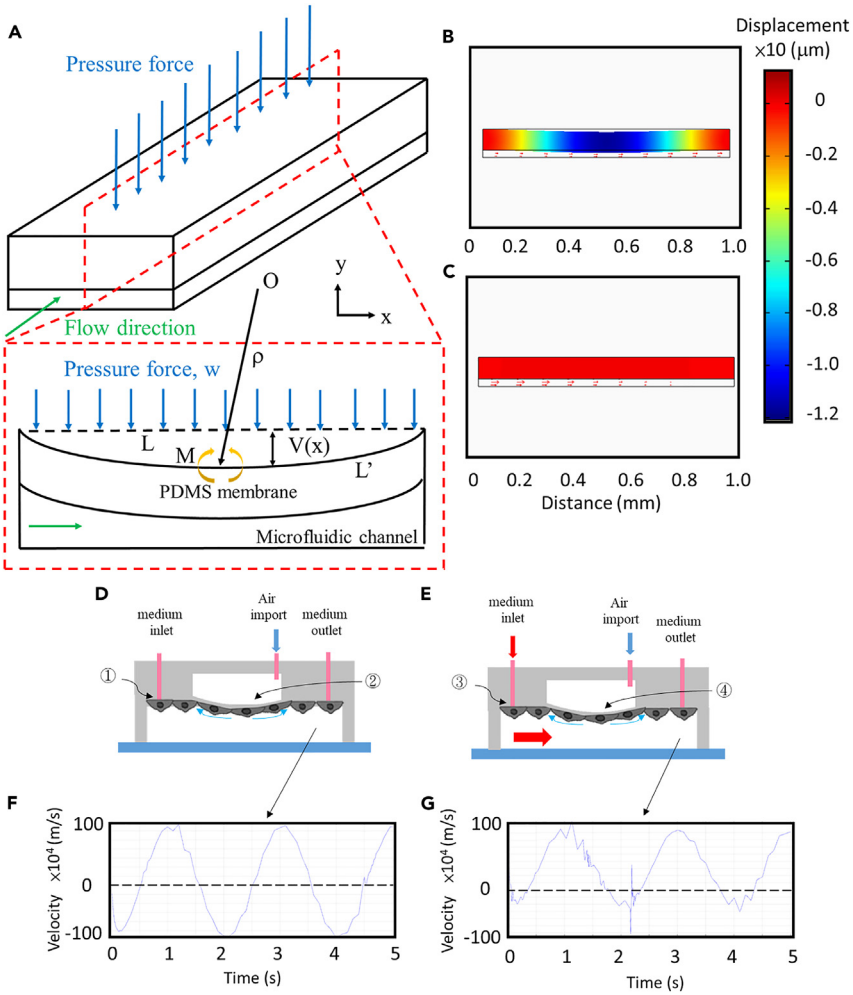

Figure 2. Simulation results

(A) Schematics of the structure of the device.

(B–E) The simulation results of pulsatile flow that is formed by coupling steady fluidic flow and cyclic PDMS deformation-induced fluidic flow (Videos S1 and S2). Pseudocolor represents stress of deformed PDMS, and arrows represent flow direction and scale in microfluidic channel. The animations of the entire simulation in a period is provided in supplemental materials including: (D) reciprocating flow induced by cyclic PDMS deformation, and (E) pulsatile flow, combination of steady fluidic flow and reciprocating flow. 1 to 4 represents different mechano-environments for BAECs, 1: reciprocating flow, 2: reciprocating flow and cyclic stretch, 3: pulsatile flow, and 4: pulsatile flow and cyclic stretch.

(F and G) The velocities of (F) reciprocating flow and (G) pulsatile flow in a period are also showed. An experimental result of the particle tracing in microfluidic channel is also realized to demonstrate pulsatile flow. The particle bouncing means backward flow that can be scaled by tuning steady flow rate.

sides were fixed, and the moving mesh was applied. The upstream of microfluidic channel was given to left side, and boundary conditions of continuity at left and right sides were set. When applying displacement at central point in a period and constant flow speed from upstream, the flow field of microfluidic channel was calculated by solving Navier-Stokes equation. The simulating results are shown in Figures 2B and 2C; (Videos S1 and S2). Therefore, different flow types, including continuous flow, reciprocating flow, and pulsatile flow can be modulated by tuning displacement and flow speed. For further experiment, the BAECs in the vessel mimicking microfluidic channel are subjected to stretch force and different flow types.

To estimate the elongation rate of PDMS membrane in one direction after deflection, we assumed the PDMS structure is a beam with length of L that is fixed supported at both end and is subjected to the uniform loading with force of w. When the internal moment M deforms the element of the beam, the beam deflects as shown in Figure 2A. The curvature, c, can be expressed as

$$\kappa = \frac{1}{\rho} = \frac{M}{EI} \quad \text{(Equation 1)}$$

where c is the radius of curvature at the point on the elastic curve, E is material's modulus of elasticity, and I is beam's moment of inertia about the neutral axis. The curvature in term of the equation of elastic curve v(x) is,

$$\kappa = \frac{1}{\rho} = \frac{d^2v(x)/dx^2}{\left[1+(dv(x)/dx)^2\right]^{3/2}} \quad \text{(Equation 2)}$$

For a small deflection, the curvature can be approximated by,

$$\kappa = \frac{1}{\rho} = \frac{d^2v(x)}{dx^2} \quad \text{(Equation 3)}$$

Therefore, the relationship between the equation of elastic curve and internal moment can be found as,

$$\frac{d^2v(x)}{dx^2} = \frac{M(x)}{EI} \quad \text{(Equation 4)}$$

The displacement at the two ends are fixed, the slope of the surface after deformation at the two ends are equal to 0, and the maximum displacement of V_{max} is at the center of the beam.

Based on calculation, if the V_{max} are given from 10 to 70 μm, the length of deformed curvature, L', will elongate 0.02%–1.2% in one direction. According to previous study,[7] the diameter change during pulse flow is around 1%–15% in the several main arteries of a man including aorta, carotid arteries, femoral arteries, and pulmonary arteries. The channel size and cell elongation in this study is corresponding to that in arterioles and partial arteries. Enlarging channel size and increasing pressure force are able to increase displacement for mimicking aorta and arteries.

(1) Continuous flow:

The syringe pump provided continuous steady flow rate to the microfluidic shearing-stretching device, and the BAECs in the microfluidic channel were subjected to fluid shear stress. The wall shear stress (τ_w) calculation was based on the Fourier series expansions and it was derived a simple approximation [38–39]:

$$\tau_w = \frac{2\mu Q}{wh^2}\left(\frac{m+1}{m}\right)(n+1) \quad \text{(Equation 5)}$$

where μ is the fluid viscosity, Q is the flow rate, w is the width of the microfluidic channel, h is the height of the microfluidic channel, and m and n are empirical constants. The wall shear stresses calculated were 138.4 and 184.5 dyn/cm^2 in this study.

(2) Cyclic stretch with reciprocating flow:

The programmable air pressure system provided periodic pressure on the microfluidic channel, which deformed and caused the BAECs to subject the cyclic stretch. COMSOL was used to simulate that the flow field in the microfluidic channel is reciprocating flow. It can find that the BAECs at the edge are not stretched, whereas the BAECs at the center are stretched. Therefore, the BAECs at the upstream and downstream were only be subjected to reciprocating flow, whereas the BAECs at the central were being subjected to both cyclic stretch and reciprocating flow as Schematics in Figure 2D. The periodic variation of flow velocity was simulated and plotted in Figure 2F.

(3) Cyclic stretch with pulsatile flow:

The syringe pump provided a continuous flow in the microfluidic channel, which also deformed by the periodic pressure from the programmable air pressure system as Figure 2E. COMSOL was used to simulate the flow field in the microfluidic channel. The periodic variation of flow velocity was simulated and plotted in Figure 2G. It was found that the BAECs at the edge were not stretched whereas the BAECs at the center

were stretched. Therefore, the BAECs at the edge were only subjected to pulsatile flow whereas the BAECs at the center were subjected to both cyclic stretch and pulsatile flow.

An experimental result of the particle tracing in microfluidic channel is also realized to demonstrate pulsatile flow. The experimental Video S3 is provided in supplementary information. In this experiment, we demonstrated the most complicate combination of the FSS, which is pulsatile flow with flow reverse that is also corresponding to the simulations shown in Figure 2G. It indicates that the system can further be used to simulate the situation of mitral insufficiency. By increasing flow rate of continuous flow, the reversal flow can be offset.

This vessel mimicking microfluidic platform showed the major advantage that the device is able to study multiple parameters by individually/simultaneously applying shearing force and stretching force. As Figure 1A, continuous flow only, the ECs received continuous shearing force. As Figure 2D, cyclic stretch only, the ECs at area 1 received reciprocating flowing force, and the ECs at area 2 received both of reciprocating flowing force and cyclic stretching force. As Figure 2E, simultaneously applying continuous flow and cyclic stretch, the ECs at area 3 received pulsatile flow only, and that at area 4 received both pulsatile flowing force and cyclic stretching force. The experimental results are shown below:

Effects of fluid shear stress and substrate stiffness

To study substrate stiffness regulated cell response when sensing fluid shear stress, we first separately cultured BAECs in PDMS substrate and glass substrate based microfluidic channel, and applied fluid shear stress for 24 h. The glass substrate was spinning-coated uncured PDMS and then baked until cured to obtain PDMS substrate. The w/wo PDMS coated glass substrate was bonded with microfluidic channels.

The Young's Modules of PDMS and glass were ~1.5 MPa[40] and 50–90 GPa, respectively, with about 10,000-folds different. Based on previously study found that the physiological elastic modulus measured by tensile test of coronary arteries obtained from healthy humans aged 25 to 50 was between 0.85 and 1.75 MPa.[41] It means that the elastic modulus of PDMS is suitable to mimic human arteries.

The suspended BAECs were separately injected into microfluidic channels with PDMS or glass substrates, incubated BAECs on the substrates in channel for 48 h to let BAECs settling down as Figures 3A and 3B, and then applied static purely FSS of 138.4 and 184.5 dyn/cm^2 for 24 h without stretching. The images were recorded every 30 min and the variation of the cell morphology was observed after 24 h.

When BAECs were cultured on PDMS substrate-based microfluidic channels, the comparison images from devices w/o applying different FSS after 24 h were shown in Figure 3C. The morphology of cells which seeding on PDMS was not aligned with the direction of fluid flow under 24 h FSS, comparing with static control. We measured the angle of stress fibers with the long-axis of the cell under static condition or under 24 h FSS, and plotted the charts to observe the angle distribution of cells (Figure 3E). On PDMS substrate, the angle distribution of stress fibers was dispersed but slightly perpendicular to FSS. The rose diagram results clearly showed that the cells seeding on PDMS did not align with the direction of fluid flow under 24 h FSS comparing to static condition.

When BAECs were cultured on glass substrate-based microfluidic channel, the comparison images from devices w/o applying different FSS after 24 h were shown in Figure 3D, which are FSS-dependent response. The angle of stress fibers with the long-axis of the cell was dispersed on treated with static condition. On FSS treatment, cells were tended to align along the direction of flow direction after 24 h FSS. Similar results were found in the rose diagram (Figure 3F). The results showed significance in the statistics, moreover, compare to the PDMS-based device, BAECs also had significance that cells tended to align along the direction of FSS with applying FSS on glass substrate.

We simulated the endothelial cells under various environmental conditions and successfully observed that the stiffness of materials affected cell morphology, most of the cells preferred to attach on the glass than PDMS substrate. Furthermore, we first separately cultured BAECs in PDMS substrate and glass substrate based microfluidic channel, to study whether substrate stiffness can regulate cell alignment under fluid shear stress (FSS). However, PDMS substrate-based microfluidic system did not show the statistical significance alignment with the direction of fluid flow under FSS 138.4 and 184.5 dyn/cm^2 up to 24 h. However, the glass-based microfluidic system tended to align along the direction of applying FSS in 24 h (Figures 3D,

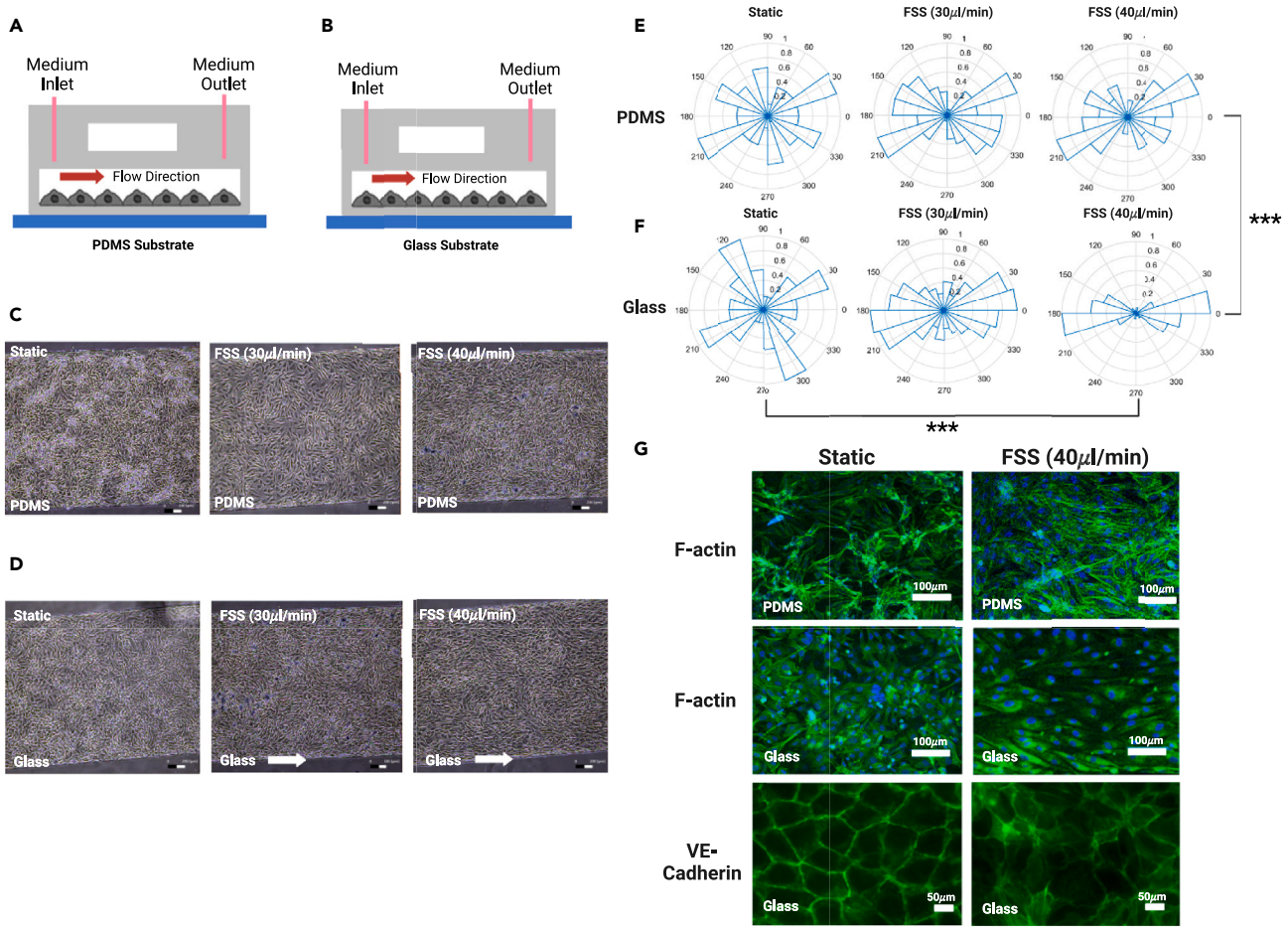

Figure 3. The angle distribution of cells adhered to the substrates of different materials

(A and B) The microfluidic device setup with (A) PDMS substrate and (B) glass substrate were revealed.

(C) The cells adhered to the PDMS under static conditions or different FSS for 24 h.

(D) The cells adhered to the Glass under static conditions or different FSS for 24 h.

(E) The rose diagram shows that the angle distribution of cells adhered to the PDMS under static conditions or different FSS for 24 h.

(F) The rose diagram shows that the angle distribution of cells adhered to the Glass under static conditions or different FSS for 24 h. The white arrow is the direction of fluid flow. All experiments were repeated 3 times for data analysis. The results are presented as mean ± standard deviation.

(G) The cells with F-actin and VE-Cadherin staining in the static status and after applying FSS for 24hrs. F-actin staining showed the fiber elongation, VE-Cadherin staining showed that cell-cell interaction was built in the microfluidic system.

3F, and 3G). In fact, when cells under the FSS over 24 h, cells might injure and de-attached from both PDMS and glass substrate because of the continuous flow and limited growth environment in microfluid channel. Owing to these limitations, when cell seeded on PDMS device over 24 h, the cell numbers were sharply decreased and we cannot confirm whether the alignment would never happen, or if it is just delayed. In contrast, cells seeded in glass substrate based microfluidic channel tend to align with the FSS in 24 h.

However, after the continuous flow, the expression level of VE-cadherin was increased compared with static control. As far as we know, the adherent junction protein VE-Cadherin was highly expressed in the polarized endothelial cells. Previous study also indicated that VE-Cadherin played a critical role in vessel growth and lumen formation.[42] Adequate concentration of VE-cadherin in cell junctions were helpful for angiogenesis.

Effects of fluid shear stress and/or cyclic stretch on cell adhesion and cytoskeleton

To investigate the changes of BAECs culturing on PDMS substrate-based microfluidic channel after different combination of mechanical stimuli, the morphological changes of the cells subjected to mechanical stretching

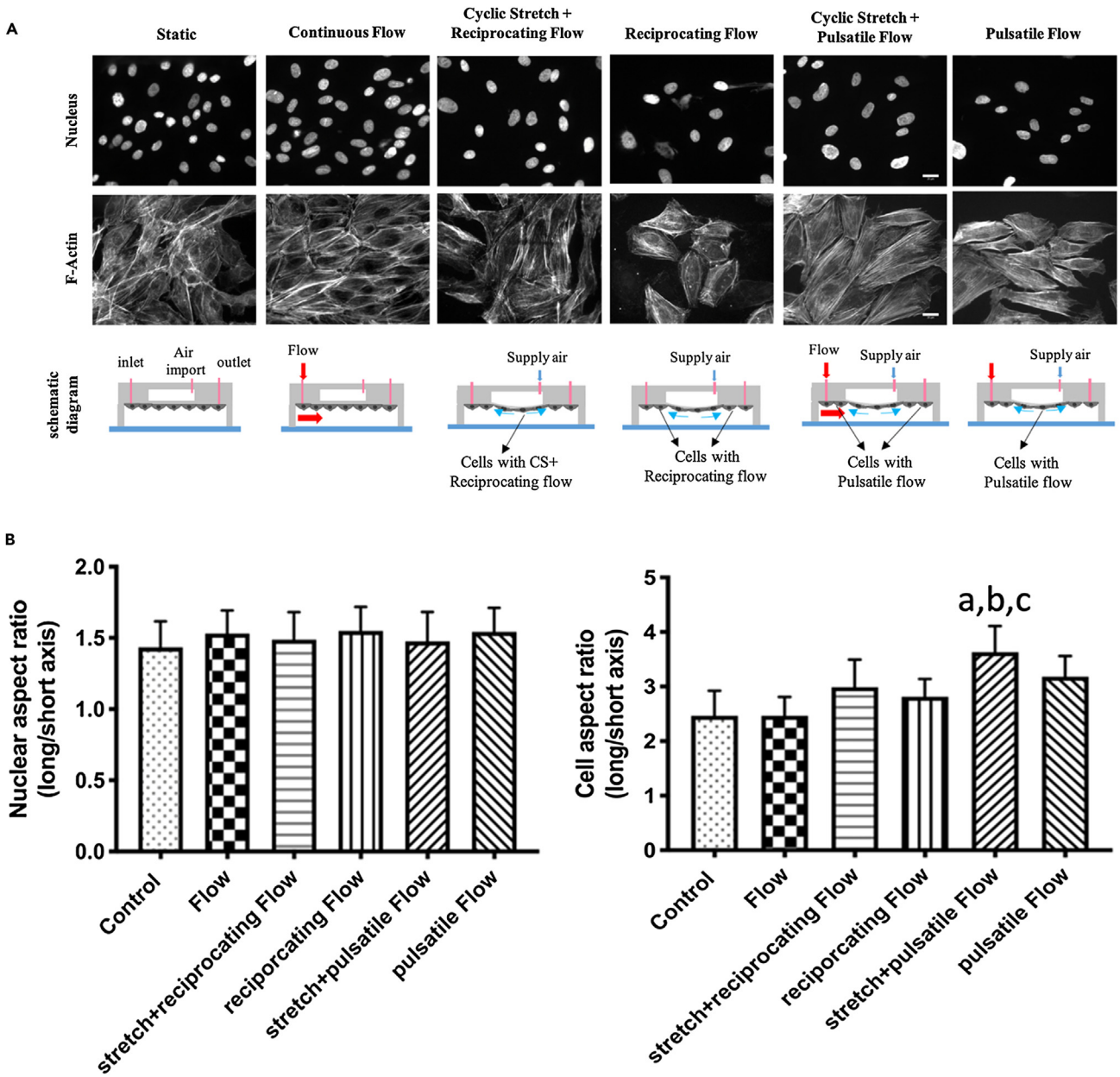

Figure 4. Effects of FSS and/or CS on the nuclear morphology and organization of F- Actin

(A) The images of cell nucleus (upper panels) and F-Actin (middle panels) under different mechanical stimulations. Lower panels indicated the organization of the devices with different mechanical stimuli. Scale bar = 20 μm. The black arrows indicate the location of the cell images in the device.

(B) The morphological changes of nucleus after BAECs were subjected to the FSS and FSS+CS as described above (n = 27, 29, 30, 21, 28, 19).

(C) The morphological changes of cell after BAECs were subjected to the FSS and FSS+CS as described above (n = 20, 18, 28, 19, 24, 16). All experiments were repeated 3 times for data analysis. The results are presented as mean ± standard deviation (a: $p < 0.005$, Control versus stretch + pulsatile flow, b: $p < 0.05$, Flow versus stretch + pulsatile flow, c: $p < 0.05$, reciprocating flow versus stretch + pulsatile flow).

(Figure 4A) was studied. Multiple cells were randomly selected for each condition, such as FSS and CS, to quantify the BAECs elongation by ImageJ. Nuclear and cell elongation was quantified by the ratio of the long axis over the short axis of a nucleus and a cell, separately. There is no significant difference in nuclei elongation under on FSS stimulus (Figure 4B), The morphology of cell was significantly elongated under the FSS+CS, and this cell elongation caused by FSS+CS was longer than that caused by FSS, whereas cell elongation increased significantly under cyclic stretch compared with the static conditions and FSS (Figure 4C).

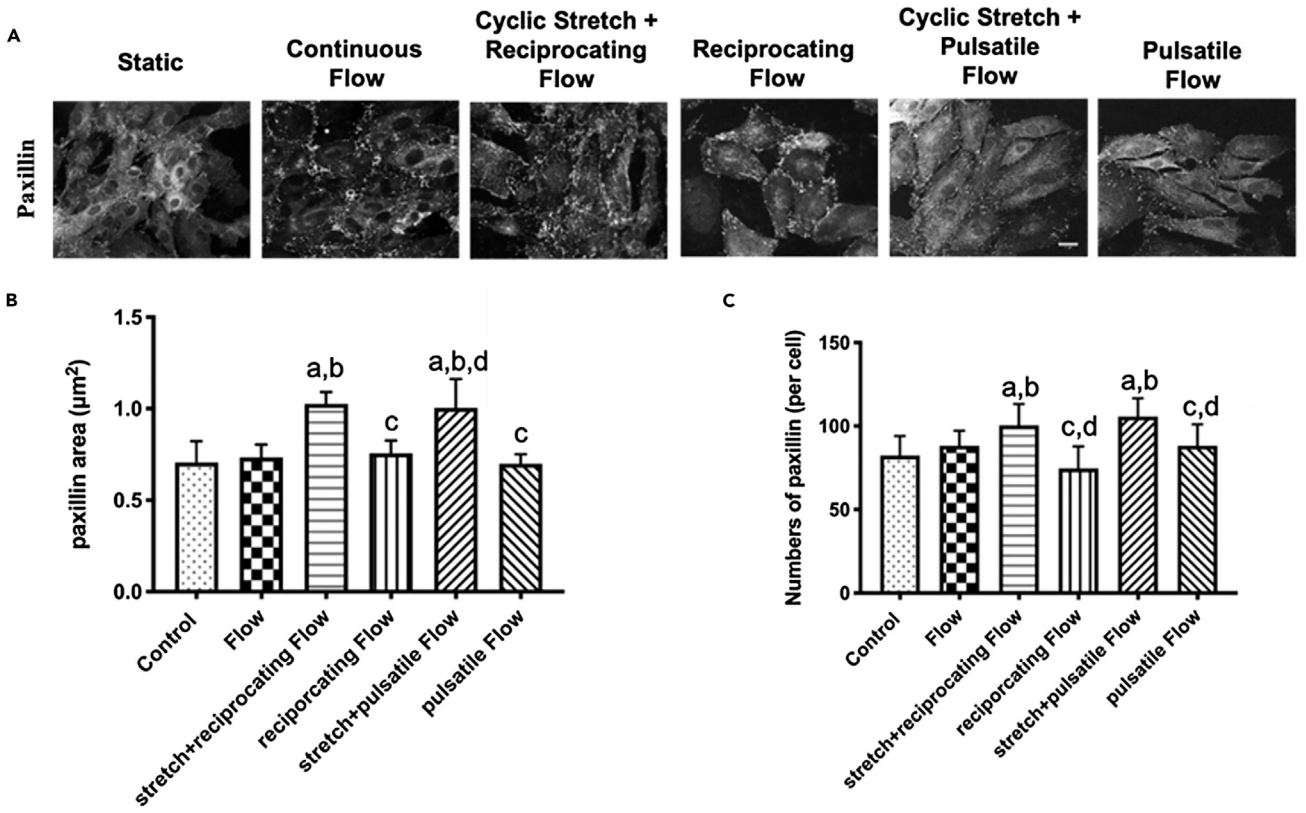

Figure 5. Effects of FSS and FSS+CS on the focal adhesions

(A) The representative images of cell staining for the paxillin under different mechanical stimulations. Scale bar = 20 μm.

(B and C) The area of paxillin after BAECs were subjected to the FSS and FSS+CS as described in Figure 4A (a: $p < 0.001$ versus Control, b: $p < 0.001$ versus Flow, c: $p < 0.001$ versus stretch+ reciprocating flow, d: $p < 0.001$ versus Pulsatile flow) (C) The number of paxillin per cell after BAECs were subjected to the FSS and FSS+CS as described in Figure 4A (n = 22, 20, 29, 32, 36, 24) All experiments were repeated 3 times for data analysis. The results are presented as mean ± standard deviation. (a: $p < 0.001$ versus Control, b: $p < 0.05$ versus Flow, b': $p < 0.005$ versus Flow, c: $p < 0.001$ versus stretch+ reciprocating flow, d: $p < 0.001$ versus stretch+ pulsatile flow).

In addition, we also measured the size and number of paxillin-marked focal adhesions after different mechanical stimuli (Figures 5A and 5B) showed that the area of paxillin-marked focal adhesions in BAECs under CS + FSS was no statistical significance compared with static or FSS. Figure 5C showed that the number of paxillin-marked focal adhesions under CS + FSS was significantly higher than that in the cells under the static flow and FSS. After the cells subjecting to these mechanical stimuli, lots of paxillin-marked focal adhesions formed at cell periphery. Also, the cell area became larger and the cell spread area increased, indicating that the area of focal adhesions was also increased.

The nuclei, F-actin, and paxillin-marked focal adhesions of BAECs were stained to observe the differences of nuclear morphology, F-actin, and the focal adhesion distribution after mechanical stimuli. Three different flow fields were applied including (1) continuous flow, (2) reciprocating flow generated by cyclic stretch, and (3) pulsatile flow generated by continuous flow coupled with cyclic stretch. The results showed that cells became elongated under cyclic stretch (Figure 6).

The BAECs were randomly arranged with a random distribution of paxillin-marked focal adhesions under static conditions. When BAECs were subjected to the FSS produced by the continuous flow, reciprocating flow or pulsatile flow, the paxillin-marked focal adhesions were distributed around the cell periphery and engaged with peripheral actin. By contrast, when BAECs were subjected to CS, the stress fibers of the cell were elongated. Paxillin-marked focal adhesions were formed and connected with the end of stress fibers.

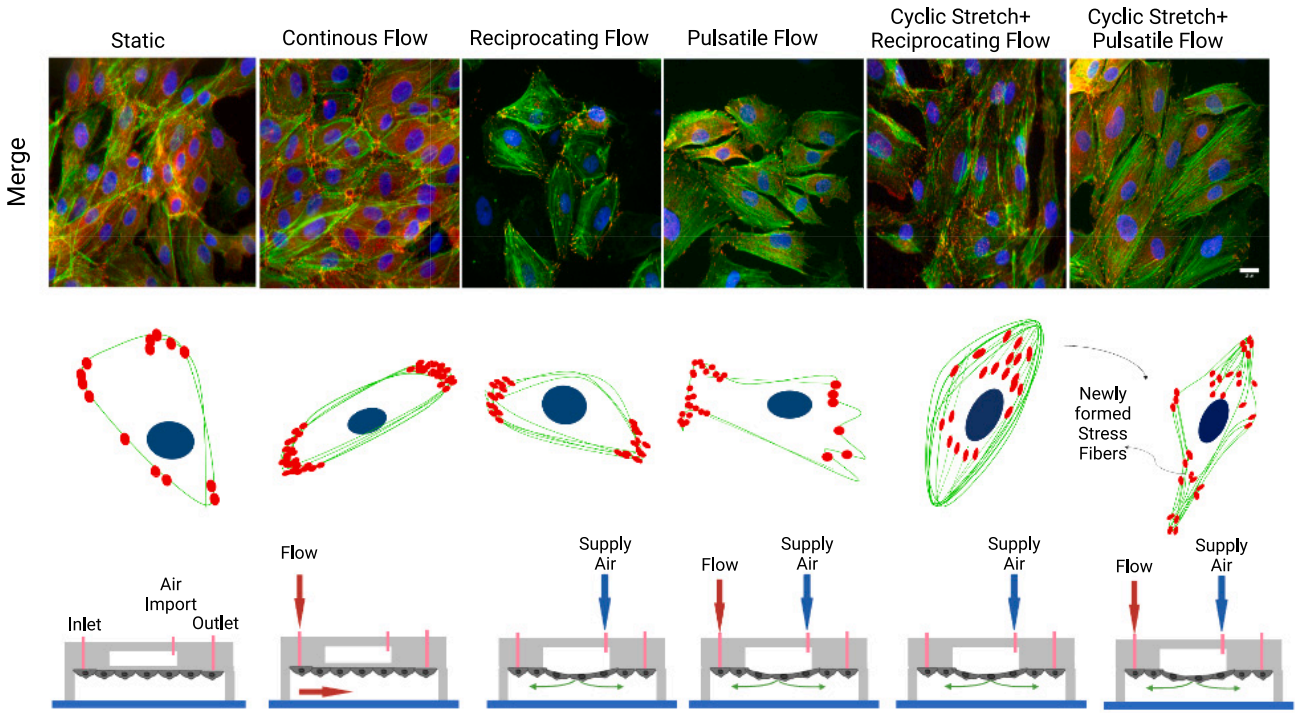

Figure 6. The merged diagram shows superimposed images from the nucleus, F-actin and paxillin

The representative fluorescence images demonstrate the localization of the paxillin and how mechanical stimuli affect localization of paxillin. Scale bar is 20 μm.

DISCUSSION

In this study, we developed a microfluidic shearing-stretching device by integrating microfluidic system and cell culture technology to mimic arterial blood vessels. This system can provide different combinations of fluid shear stress and cyclic stretch. We concluded that under the same flow condition, the cell alignment can be changed when culturing on the different stiffness of substrate materials in 24 h. When BAECs were seeded in the PDMS device, they organized their adherent junction formation after 48 h culture. As (the picture) showed in Figures 3C and 3D. Furthermore, the adherent junction was stained in Figure 3G after applying FSS for 24 h. When cells under the FSS for 24 h, some cells might injure and de-attached from the substrate because of the continuous flow and growth limitation in the microchannel. When cell seeded on PDMS device over 24 h, the cell numbers were sharply decreased and cannot confirm whether the alignment would never happen, or if it is just delayed. But the cell which seeded in glass substrate based microfluidic channel tend to align with the FSS in 24 h.

This device could also provide different mechanical stimuli to endothelial cells and regulate endothelial cell behavior. For instance, under the CS + FSS, the morphological of cells were changed (Figure 4C), the number of focal adhesion protein were significantly increased under the cyclic stretch with reciprocating flow or pulsatile flow (Figure 5C). Moreover, when cells were subjected to CS + FSS, reciprocating flow or pulsatile flow, the paxillin-marked focal adhesion proteins were distributed around the cell periphery and interacted with peripheral actin (Figure 6).

In the previous study, indicated that under the stimulating through the shear force of flow field, paxillin and p130 ^{CAS} were phosphorylated and formed paxillin-p130 ^{CAS}-DOCK180/ELMO complex with DOCK180 and ELMO.[43] This complex effectively activated Rac1 and played a critical role on cell migration. This study uses the shear stress of the flow field to observe the attachment of endothelial cells. According to this finding, the research can be found that the microfluidic device in this study can effectively affect the state of the endothelial cells through the shear stress of the flow field. Recently the research also indicated that shear stress in stable laminar flow will cause inflammation of endothelial

cells and atherosclerosis.[44] Therefore, this study will be able to treat cardiovascular diseases such as atherosclerosis by increasing microchannel bending or bifurcation, contribute to preventive medical care.

Limitations of the study

By observing the behavior of cells under mechanical stimuli, we can explore the cellular mechanics, drug screening with this device in the future. For example, to investigate thrombosis, one of the common cardiovascular diseases, vessel-on-a-chip can be created. Human endothelial cells (EC) can be seeded into this microchannels, these chips can stimulate the blood vessel operation, mimic the arterial environment including pulsatile flow and dynamic stretch. Furthermore, cell behaviors in the system can be monitored in real-time.

STAR★METHODS

Detailed methods are provided in the online version of this paper and include the following:

- KEY RESOURCES TABLE
- RESOURCE AVAILABILITY
  - Lead contact
  - Materials availability
  - Data and code availability
- EXPERIMENTAL MODEL AND SUBJECT DETAILS
- METHOD DETAILS
  - Device design and fabrication
  - Cell culture
  - Immunostaining
- QUANTIFICATION AND STATISTICAL ANALYSIS

SUPPLEMENTAL INFORMATION

Supplemental information can be found online at https://doi.org/10.1016/j.isci.2023.106927.

ACKNOWLEDGMENTS

This work was supported by the Ministry of Science and Technology of Taiwan under grant numbers MOST 110-2636-E-038 -004 and 106-2218-E-038 -003. This work also got financial support by National Laboratory Animal Center (NLAC), NARLabs, Taiwan, under grant numbers NLAC-S-111030. We would like to thank the the Semiconductor Fabrication Lab of the Consortia of Key Technologies and the Nano-Electro-Mechanical-System Research Center, National Taiwan University for facility support. We would also like to thank the Prof. Chia-Ching Wu from National Cheng Kung University providing Bovine Aortic Endothelial Cells, and Prof. Yang-Kao Wang from National Cheng Kung University for technical supporting and consulting.

AUTHOR CONTRIBUTIONS

P-Y.C. and H-Y.H.: Methodology, Investigation, Data curation, Writing – original draft preparation. P-S.C. and P-W.W.: Methodology, Investigation, Data curation. Writing – original draft preparation. M-C.W. and Y-Q.C.: Methodology, Investigation, Data curation. J-C.K. and K-C.W.: Conceptualization, Project administration, Funding acquisition. Y-J.F.: Conceptualization, Methodology, Data curation, Writing – review and editing, Project administration, Funding acquisition, All authors have read and agreed to the published version of the manuscript.

DECLARATION OF INTERESTS

There are no conflicts to declare.

Received: December 21, 2021
Revised: October 24, 2022
Accepted: May 16, 2023
Published: May 19, 2023

REFERENCES

1. Sumpio, B.E., Riley, J.T., and Dardik, A. (2002). Cells in focus: endothelial cell. Int. J. Biochem. Cell Biol. *34*, 1508–1512.

2. Chappell, D.C., Varner, S.E., Nerem, R.M., Medford, R.M., and Alexander, R.W. (1998). Oscillatory shear stress stimulates adhesion molecule expression in cultured human endothelium. Circ. Res. *82*, 532–539.

3. Punchard, M.A., O'Cearbhaill, E.D., Mackle, J.N., McHugh, P.E., Smith, T.J., Stenson-Cox, C., and Barron, V. (2009). Evaluation of human endothelial cells post stent deployment in a cardiovascular simulator in vitro. Ann. Biomed. Eng. *37*, 1322–1330.

4. Benbrahim, A., L'Italien, G.J., Milinazzo, B.B., Warnock, D.F., Dhara, S., Gertler, J.P., Orkin, R.W., and Abbott, W.M. (1994). A compliant tubular device to study the influences of wall strain and fluid shear stress on cells of the vascular wall. J. Vasc. Surg. *20*, 184–194.

5. Caille, N., Tardy, Y., and Meister, J.-J. (1998). Assessment of strain field in endothelial cells subjected to uniaxial deformation of their substrate. Ann. Biomed. Eng. *26*, 409–416.

6. Peng, X., Recchia, F.A., Byrne, B.J., Wittstein, I.S., Ziegelstein, R.C., and Kass, D.A. (2000). In vitro system to study realistic pulsatile flow and stretch signaling in cultured vascular cells. Am. J. Physiol. Cell Physiol. *279*, C797–C805.

7. Young, E.W.K., and Simmons, C.A. (2010). Macro-and microscale fluid flow systems for endothelial cell biology. Lab Chip *10*, 143–160.

8. Gahan, P.B. (2002). Molecular biology of the cell (4th edn) B. Alberts, A. Johnson, J. Lewis, K. Roberts and P. Walter (eds), Garland Science, 1463 pp., ISBN 0-8153-4072-9 (paperback) (2002). Cell Biochem. Funct. *23*, 150. https://doi.org/10.1002/cbf.1142.

9. Hynes, R.O. (1992). Integrins: versatility, modulation, and signaling in cell adhesion. Cell *69*, 11–25.

10. Shyy, J.Y.-J., and Chien, S. (2002). Role of integrins in endothelial mechanosensing of shear stress. Circ. Res. *91*, 769–775.

11. Lamalice, L., Le Boeuf, F., and Huot, J. (2007). Endothelial cell migration during angiogenesis. Circ. Res. *100*, 782–794.

12. Thi, M.M., Tarbell, J.M., Weinbaum, S., and Spray, D.C. (2004). The role of the glycocalyx in reorganization of the actin cytoskeleton under fluid shear stress: a "bumper-car" model. Proc. Natl. Acad. Sci. USA *101*, 16483–16488.

13. Cotran, R.S., and Pober, J.S. (1990). Cytokine-endothelial interactions in inflammation, immunity, and vascular injury. J. Am. Soc. Nephrol. *1*, 225–235.

14. Ebnet, K., and Vestweber, D. (1999). Molecular mechanisms that control leukocyte extravasation: the selectins and the chemokines. Histochem. Cell Biol. *112*, 1–23. https://doi.org/10.1007/s004180050387.

15. Pearson, J.D. (1999). Endothelial cell function and thrombosis. Baillieres Best Pract. Res. Clin. Haematol. *12*, 329–341. https://doi.org/10.1053/beha.1999.0028.

16. van Hinsbergh, V.W.M. (2012). Endothelium–role in regulation of coagulation and inflammation. Semin. Immunopathol. *34*, 93–106. https://doi.org/10.1007/s00281-011-0285-5.

17. Wu, K.K., and Thiagarajan, P. (1996). Role of endothelium in thrombosis and hemostasis. Annu. Rev. Med. *47*, 315–331. https://doi.org/10.1146/annurev.med.47.1.315.

18. Yau, J.W., Teoh, H., and Verma, S. (2015). Endothelial cell control of thrombosis. BMC Cardiovasc. Disord. *15*, 130. https://doi.org/10.1186/s12872-015-0124-z.

19. Mackman, N. (2008). Triggers, targets and treatments for thrombosis. Nature *451*, 914–918. https://doi.org/10.1038/nature06797.

20. Stathopoulos, N.A., and Hellums, J.D. (1985). Shear stress effects on human embryonic kidney cells in Vitro. Biotechnol. Bioeng. *27*, 1021–1026. https://doi.org/10.1002/bit.260270713.

21. Nomura, H., Ishikawa, C., Komatsuda, T., Ando, J., and Kamiya, A. (1988). A disk-type apparatus for applying fluid shear stress on cultured endothelial cell. Biorheology *25*, 461–470. https://doi.org/10.3233/bir-1988-25307.

22. Sumpio, B.E., Banes, A.J., Link, G.W., and Iba, T. (1990). Modulation of endothelial cell phenotype by cyclic stretch: inhibition of collagen production. J. Surg. Res. *48*, 415–420. https://doi.org/10.1016/0022-4804(90)90005-m.

23. Busse, R., and Fleming, I. (1998). Pulsatile stretch and shear stress: physical stimuli determining the production of endothelium-derived relaxing factors. J. Vasc. Res. *35*, 73–84. https://doi.org/10.1159/000025568.

24. Kaunas, R., Usami, S., and Chien, S. (2006). Regulation of stretch-induced JNK activation by stress fiber orientation. Cell. Signal. *18*, 1924–1931. https://doi.org/10.1016/j.cellsig.2006.02.008.

25. Takeda, H., Komori, K., Nishikimi, N., Nimura, Y., Sokabe, M., and Naruse, K. (2006). Bi-phasic activation of eNOS in response to uni-axial cyclic stretch is mediated by differential mechanisms in BAECs. Life Sci. *79*, 233–239. https://doi.org/10.1016/j.lfs.2005.12.051.

26. Ives, C.L., Eskin, S.G., and McIntire, L.V. (1986). Mechanical effects on endothelial cell morphology: in vitro assessment. In Vitro Cell. Dev. Biol. Plant *22*, 500–507. https://doi.org/10.1007/bf02621134.

27. Ives, C.L., Eskin, S.G., McIntire, L.V., and DeBakey, M.E. (1983). The importance of cell origin and substrate in the kinetics of endothelial cell alignment in response to steady flow. Trans. Am. Soc. Artif. Intern. Organs *29*, 269–274.

28. Shikata, Y., Rios, A., Kawkitinarong, K., DePaola, N., Garcia, J.G.N., and Birukov, K.G. (2005). Differential effects of shear stress and cyclic stretch on focal adhesion remodeling, site-specific FAK phosphorylation, and small GTPases in human lung endothelial cells. Exp. Cell Res. *304*, 40–49. https://doi.org/10.1016/j.yexcr.2004.11.001.

29. Birukov, K.G., Birukova, A.A., Dudek, S.M., Verin, A.D., Crow, M.T., Zhan, X., DePaola, N., and Garcia, J.G.N. (2002). Shear stress-mediated cytoskeletal remodeling and cortactin translocation in pulmonary endothelial cells. Am. J. Respir. Cell Mol. Biol. *26*, 453–464. https://doi.org/10.1165/ajrcmb.26.4.4725.

30. Birukov, K.G., Jacobson, J.R., Flores, A.A., Ye, S.Q., Birukova, A.A., Verin, A.D., and Garcia, J.G.N. (2003). Magnitude-dependent regulation of pulmonary endothelial cell barrier function by cyclic stretch. Am. J. Physiol. Lung Cell Mol. Physiol. *285*, L785–L797. https://doi.org/10.1152/ajplung.00336.2002.

31. Toda, M., Yamamoto, K., Shimizu, N., Obi, S., Kumagaya, S., Igarashi, T., Kamiya, A., and Ando, J. (2008). Differential gene responses in endothelial cells exposed to a combination of shear stress and cyclic stretch. J. Biotechnol. *133*, 239–244. https://doi.org/10.1016/j.jbiotec.2007.08.009.

32. Folch, A., and Toner, M. (2000). Microengineering of cellular interactions. Annu. Rev. Biomed. Eng. *2*, 227–256. https://doi.org/10.1146/annurev.bioeng.2.1.227.

33. Khademhosseini, A., Langer, R., Borenstein, J., and Vacanti, J.P. (2006). Microscale technologies for tissue engineering and biology. Proc. Natl. Acad. Sci. USA *103*, 2480–2487. https://doi.org/10.1073/pnas.0507681102.

34. Whitesides, G.M., Ostuni, E., Takayama, S., Jiang, X., and Ingber, D.E. (2001). Soft lithography in biology and biochemistry. Annu. Rev. Biomed. Eng. *3*, 335–373. https://doi.org/10.1146/annurev.bioeng.3.1.335.

35. Zheng, W., Jiang, B., Wang, D., Zhang, W., Wang, Z., and Jiang, X. (2012). A microfluidic flow-stretch chip for investigating blood vessel biomechanics. Lab Chip *12*, 3441–3450. https://doi.org/10.1039/c2lc40173h.

36. Xia, Y., and Whitesides, G.M. (1998). Soft LITHOGRAPHY. Annu. Rev. Mater. Sci. *28*, 153–184. https://doi.org/10.1146/annurev.matsci.28.1.153.

37. McDonald, J.C., and Whitesides, G.M. (2002). Poly(dimethylsiloxane) as a material for fabricating microfluidic devices. Acc. Chem. Res. *35*, 491–499. https://doi.org/10.1021/ar010110q.

38. Shah, R.K., and London, A.L. (1978). Laminar Flow Forced Convection in Ducts: A Source

Book for Compact Heat Exchanger Analytical Data (Academic press).

39. Dobrin, P.B. (1978). Mechanical properties of arteries. Physiol. Rev. *58*, 397–460. https://doi.org/10.1152/physrev.1978.58.2.397.

40. Sales, F.C., Ariati, R.M., Noronha, V.T., and Ribeiro, J.E. (2022). Mechanical characterization of PDMS with different mixing ratios. Int. J. Struct. Integr. *37*, 383–388. https://doi.org/10.1016/j.prostr.2022.01.099.

41. Karimi, A., Navidbakhsh, M., Shojaei, A., and Faghihi, S. (2013). Measurement of the uniaxial mechanical properties of healthy and atherosclerotic human coronary arteries. Mater. Sci. Eng. C *33*, 2550–2554. https://doi.org/10.1016/j.msec.2013.02.016.

42. Cao, J., Ehling, M., März, S., Seebach, J., Tarbashevich, K., Sixta, T., Pitulescu, M.E., Werner, A.-C., Flach, B., Montanez, E., et al. (2017). Polarized actin and VE-cadherin dynamics regulate junctional remodelling and cell migration during sprouting angiogenesis. Nat. Commun. *8*, 2210. https://doi.org/10.1038/s41467-017-02373-8.

43. Zaidel-Bar, R., Kam, Z., and Geiger, B. (2005). Polarized downregulation of the paxillin-p130CAS-Rac1 pathway induced by shear flow. J. Cell Sci. *118*, 3997–4007. https://doi.org/10.1242/jcs.02523.

44. Cheng, C.K., Lin, X., Pu, Y., Tse, J.K.Y., Wang, Y., Zhang, C.-L., Cao, X., Lau, C.W., Huang, J., He, L., et al. (2023). SOX4 is a novel phenotypic regulator of endothelial cells in atherosclerosis revealed by single-cell analysis. J. Adv. Res. *43*, 187–203. https://doi.org/10.1016/j.jare.2022.02.017.

45. Fan, Y.-J., Hsiao, Y.-C., Weng, Y.-L., Chen, Y.-H., Chiou, P.-Y., and Sheen, H.-J. (2020). Development of a parallel three-dimensional microfluidic device for high-throughput cytometry. Sens. Actuators B Chem. *320*, 128255. https://doi.org/10.1016/j.snb.2020.128255.

46. Fan, Y.-J., Huang, M.-Z., Hsiao, Y.-C., Huang, Y.-W., Deng, C.-Z., Yeh, C., Husain, R.A., and Lin, Z.-H. (2020). Enhancing the sensitivity of portable biosensors based on self-powered ion concentration polarization and electrical kinetic trapping. Nano Energy *69*, 104407. https://doi.org/10.1016/j.nanoen.2019.104407.

47. Fan, Y.-J., Deng, C.-Z., Chung, P.-S., Tian, W.-C., and Sheen, H.-J. (2018). A high sensitivity bead-based immunoassay with nanofluidic preconcentration for biomarker detection. Sens. Actuators B Chem. *272*, 502–509. https://doi.org/10.1016/j.snb.2018.05.141.

48. Kung, Y.-C., Huang, K.-W., Fan, Y.-J., and Chiou, P.-Y. (2015). Fabrication of 3D high aspect ratio PDMS microfluidic networks with a hybrid stamp. Lab Chip *15*, 1861–1868.

STAR★METHODS

KEY RESOURCES TABLE

REAGENT or RESOURCE	SOURCE	IDENTIFIER
Antibodies		
phalloidin-TRITC	Thermo Fisher Scientific	Cat#R415; RRID: AB_2572408
Hoechst33342	Thermo Fisher Scientific	Cat#H3570
VE-cadherin	Santa Cruz	Cat#SC9989; RRID: AB_2077957
anti-mouse IgG Alexa Flour 488 secondary antibody	Invitrogen	Cat#A-11001; RRID: AB_253406
Chemicals, peptides, and recombinant proteins		
Fibronectin	Sigma-Aldrich	Cat#11051407001
Collagen	Thermo Fisher Scientific	Cat#A1048301
Experimental models: Cell lines		
Bovine Aorta Endothelial Cells	Dr. Chia-Ching Wu, National Cheng Kung University, Tainan, Taiwan	N/A
Software and algorithms		
Micro-Manager 1.4 software	Leica	https://micro-manager.org/Micro-Manager_Version_Archive
GraphPad Prism 9	GraphPad Software	https://www.graphpad.com/
ImageJ	Schneider et al.	https://imagej.nih.gov/ij/
COMSOL	COMSOL Inc.	https://www.comsol.com/

RESOURCE AVAILABILITY

Lead contact

Further information and requests for resources and reagents should be directed to and will be fulfifilled by the lead contact, Yu-Jui Fan (ray.yj.fan@tmu.edu.tw)

Materials availability

This study did not generate new unique reagents.

Data and code availability

- All data produced in this study are included in the published article and its supplemental information, or are available from the lead contact upon request.
- This paper does not report original code.
- Any additional information required to reanalyze the data reported in this paper is available from the lead contact upon request.

EXPERIMENTAL MODEL AND SUBJECT DETAILS

The experimental system, shown in Figure S1, consisted of a programmable air pressure control system, a syringe pump, and a stage top incubator (STR, Tokai Hit) for culturing cells on microscope. The inlet and outlet of microfluidic channel were connected to a medium-filled syringe, and a syringe pump was used to provide a continuously fluid flow in the microfluidic channel. The programmable air pressure system was composed of a function generator and control system. When supplying a sinusoid wave with frequency of 1 Hz to relay in control system by functional generator, the switching valve will cyclically switch the air chamber of device to connect with pressurized air source and atmosphere the air chamber. Initially, the microfluidic channel at releasing state, the channel wall remained flat, and endothelial cells adhered at PDMS

surface to form a monolayer. When the air chamber was at pressurizing state, the adhered cells at the PDMS wall between air chamber and microfluidic channel were stretched in three dimensional directions. Therefore, the air chamber was cyclically pressurized and released and the cells will receive cyclic stretch force.

METHOD DETAILS

Device design and fabrication

The microfluidic shearing-stretching device as Figures 1C and 1D consisted of three parts: a glass (width 25.4 mm, length 38 mm, height 1 mm), a microfluidic channel (width 1 mm, length 18 mm, height 82 μm), and an air chamber (width 2 mm, length 10 mm, height 55 μm). The Polydimethylsiloxane (PDMS) was used for the fabrication of microfluidic channel and the air chamber. PDMS possessed the characteristics of optical transparency, high biocompatibility, high elasticity and good permeability and demonstrated the ability to construct microfluidic device as well as multi-layer microfluidic device[45–48] through soft lithography. Firstly, the master molds for fabricating air chamber and microfluidic channel were made by using traditional photolithography to pattern SU-8 on silicon wafers, separately. Secondly, PDMS was poured onto the silicon wafer and cured for 1 hour at 70°C. The replica of PDMS was then peeled off from the SU-8 mold. The PDMS microfluidic channel and PDMS air chamber were bonded onto the glass substrate, layer-by-layer by using oxygen plasma-pre-treated surface.

Cell culture

In this study, primary bovine aortic endothelial cells (BAECs, a kind gift from Dr. Chia-Ching Wu, National Cheng Kung University, Tainan, Taiwan) were used. They were cultured in in low glucose Dulbecco's Modified Eagle Medium, (DMEM, Gibco), supplemented with 10% fetal bovine serum (GIBCO), 1x penicillin/streptomycin. Only early passage cells (<P8) were used in the study. When density of BAECs reached a confluence about 70–80%, the adhered BAECs were washed twice with PBS and suspended by trypsin-EDTA (0.25%-2 mM). The suspended cells were adjusted to the density of 107 cells/ml, and then injected in to microfluidic channels. Before delivering cells into microfluidic channel, fibronectin (100 μg/ml, Sigma-Aldrich) was used to coat inner PDMS surface of microfluidic channel for 30 min. The suspended BAECs were filled with microfluidic shearing-stretching device and incubated at 37°C for 12 h.

Immunostaining

After experiments, the cells were fixed with 4% paraformaldehyde (PFA), permeablilized with 2% Triton X-100 (Sigma-Aldrich) and then soaked in blocking buffer (SuperBlock, Thermo Fisher Scientific) at room temperature. The cells were then incubated with diluted primary antibody in the blocking buffer were incubated overnight at 4 °C and then incubated with diluted secondary antibody-conjugated with fluorephores. The F-actin was stained with phalloidin-TRITC (Thermo Fisher Scientific) and nuclei were stained with Hoechst33342. The fluorescence images were obtained using a microscope (DMRBE, Leica) coupled with a 40×, NA = 1.0 objective lens (Leica) and an 512B EMCCD (Andor) operated by Micro-Manager 1.4 software (Leica). To detect adherent junction of endothelial cells, primary antibody vascular endothelial cadherin (VE-cadherin,1:100, Santa Cruz) were used, followed by an anti-mouse IgG Alexa Flour 488 secondary antibody (1:500 Invitrogen). Hochest 33342 was used to stain the nucleus of BAECs.

QUANTIFICATION AND STATISTICAL ANALYSIS

All data are presented as mean ± standard error (SEM). p values were obtained from 2 statistical method: Two-sided paired T-tests or One-way Analysis of Variance (ANOVA) using GraphPad Prism 9. Two-sided paired T-tests were used for comparison between PDMS and Glass groups (Figure 3). ANOVA with Tukey's post-hoc test was used to compare the results with three or more groups under different flow and stretch conditions (Figures 4 and 5).